Efficient Particle Analysis

Mastering Protein and Polysorbate Detection in Biologic Formulations





Expose Hidden Dangers with Automated Particle Characterization

Hidden and dangerous aggregates can jeopardize your protein formulations. Halo Labs' Aura is the first and only solution to detect and characterize contaminants and stability, lighting the way to safer biologics.

Shine a light on the unseen: www.halolabs.com



Efficient Particle Analysis

Mastering Protein and Polysorbate Detection in Biologic Formulations

- O5 Combatting Therapeutic-Protein Aggregation
- Rapidly Distinguish Protein from Non-Protein Particles in Biologic Formulations
- 21 Direct, Non-Destructive Analysis of Subvisible Particles
- High-Throughput Detection of Degraded Polysorbate in Biological Formulations with FMM
- Protein Degradation and Particle Formation Control Strategies





Welcome Letter

Navigating the development and manufacturing of biopharmaceuticals is complex, especially when it comes to ensuring that drug formulations are stable and effective. A key challenge lies in detecting and characterizing subvisible particles (SVPs). Ranging from 1 µm to 100 µm in size, these tiny particles can cause severe health issues, from clogging capillaries to sparking life-threatening immune reactions.

Traditional methods for analyzing subvisible particles, such as light obscuration (LO) and flow imaging (FI), have limitations that make accurate particle identification difficult. LO counts particles, but cannot differentiate between particle types due to its reliance on low refractive index contrast. On the other hand, FI provides more detailed images and morphological data but struggles to fully identify the chemical makeup of particles. This inability to distinguish proteins from plastics or degraded polysorbates only adds complexity, underscoring the need for more sophisticated solutions.

Regulatory agencies now expect drug manufacturers to employ multiple, orthogonal methods to supplement traditional compendial techniques. Among these advanced techniques is Fluorescence Membrane Microscopy (FMM), a breakthrough technology exclusively available on Aura® particle analyzers. FMM offers high-throughput, low-volume identification of subvisible particles, providing an ultra-fast, 100% sampling efficiency. It can characterize everything from a single protein aggregate to tens of millions of particles across samples in under two hours.

In this eBook, we will explore how researchers can address these challenges through innovative techniques that go beyond simple particle counting and provide deep insights needed for the safe and effective development of biopharmaceuticals.



Combatting Therapeutic-Protein Aggregation



ioprocessors must minimize the aggregation of therapeutic proteins, but that's not an easy task. Proteins can aggregate during any step from manufacturing to administering a drug. "The aggregation results in an irreversible drug loss and also leads to an increase in the risk of immunogenicity," says Lalit Pandey, PhD, associate professor of biosciences and bioengineering at the Indian Institute of Technology Guwahati, India. "The aggregated proteins have also been associated with various protein-deposition diseases, like amyloidosis."

In a recent review article, Pandey explained that chemical, environmental, and mechanical factors such as salt levels, pH, and shear—can cause aggregation. "These factors induce the unfolding of proteins, which exposes sites for non-specific protein interactions, leading to the formation of higher-order structures, such as dimers, oligomers, and aggregates," he says.

Aggregation can occur across the entire process of making a therapeutic protein. In upstream



bioprocessing, cell growth and protein stability depend on many factors and conditions, including aeration, agitation, antifoam agents, osmolarity, pH, and temperature.

"This poses another challenge in bioprocessing to tune the parameters so as to optimize the product formation without inducing the aggregation," Pandey explains. "For example, the optimum temperature for cell growth may affect the stability of therapeutic proteins." A protein's stability even depends on interactions with surfaces of bioreactors and pipes.

In addition, Pandey points out steps in downstream bioprocessing that can impact aggregation. For example, "elution buffers of different pH and ionic strength are used in chromatographic separations," he says, and that can trigger aggregation. Bioprocessors also vary pH and ionic strength in viral inactivation and to neutralize antibodies. Aggregation can also arise from mechanical stresses in filtration and thermal stress in freeze-thaw cycles.

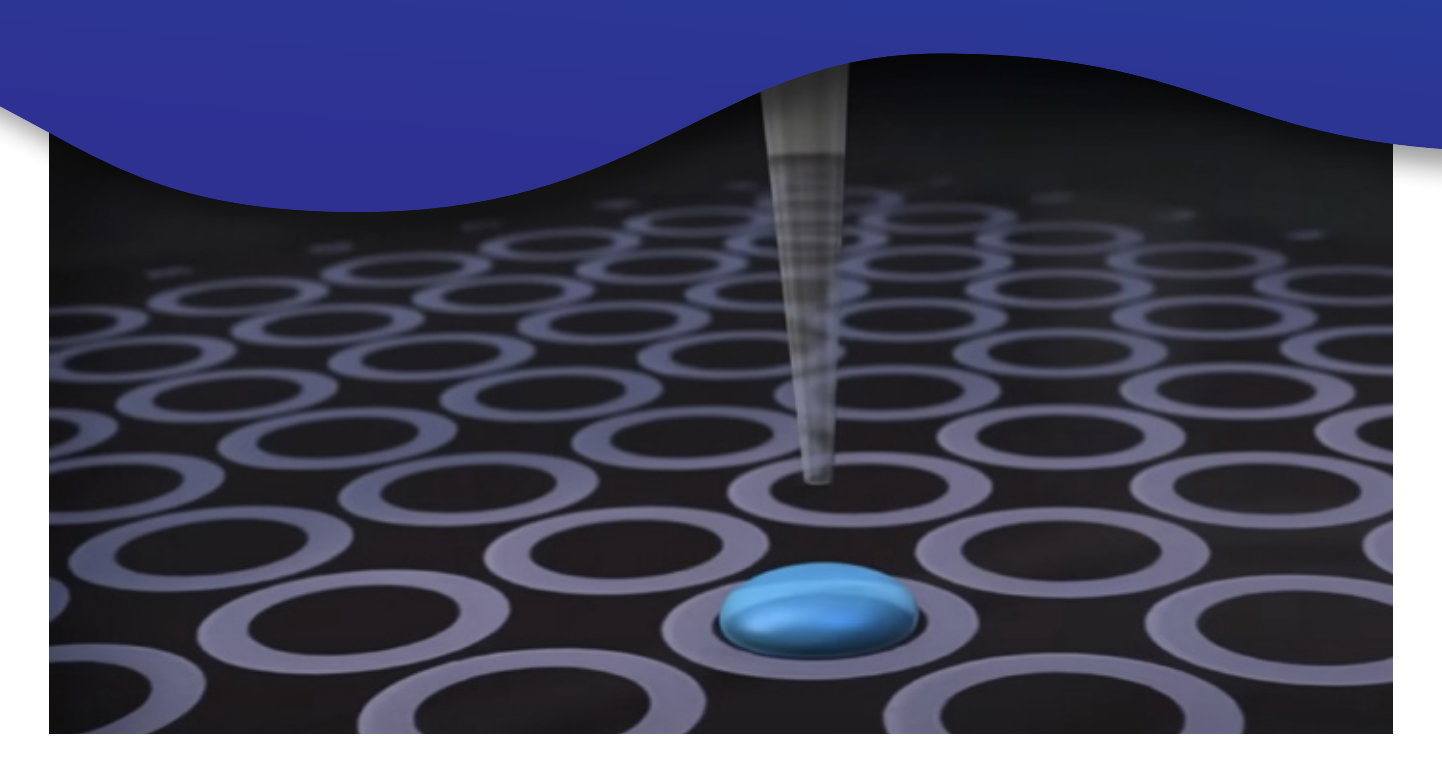
The type of ionic bonding can reduce or drive aggregation. "The spontaneous binding of ions with exothermic sites has been found to stabilize the conformation and inhibit aggregation, and the endothermic binding of ions with proteins disrupts the stabilized structure and accelerates the process of aggregation," Pandey says. "An understanding of the binding behavior of the ions with protein can help in regulating the molar concentrations of ions to control the aggregation."

A bioprocessor can minimize aggregation in various ways. "A buffer should be carefully selected for a particular therapeutic protein in order to inhibit a significant change in conformation," Pandey advises. Other processing steps offer other opportunities to reduce aggregation. As examples, Pandey notes that "fast freezing rates inhibit product aggregation," and "modifications of the contacting surfaces are being applied to inhibit or minimize non-specific protein-surface interactions," adding that in situ analysis of subvisible particles and removing them can also reduce aggregation.

As scientists learn more about protein aggregation, bioprocessors must address more parameters to minimize the problem. Consequently, "the stability of therapeutic proteins is still a challenge," states Pandey.



Rapidly Distinguish Protein from Non-Protein Particles in Biologic Formulations



Introduction

ubvisible particles (1 μm–100 μm) are a critical quality attribute for biologics and an indicator of stability. The presence of protein aggregates can limit a product's shelf life and are a key indicator of the potential immunogenicity of a drug. The FDA suggests that, "strategies to minimize aggregate formation should be developed as early as feasible in product development." Subvisible particles can come from several sources: (1) aggregation of the protein API, (2) degraded excipients and other particles present in the container system, or (3) manufacturing, packaging and other external contaminants². Identifying and quantifying the inherent particle population is crucial to monitoring stability and promoting long term-efficacy.

Current subvisible analysis techniques make accurate particle identification virtually impossible. Light obscuration (LO) is a low refractive index contrast particle counting method which cannot distinguish between different particle types. Flow imaging (FI) techniques provide more information than LO, including particle images, morphological parameters and optical characteristics of particles. However, none of these features definitively identify the type of particle imaged. Flow imagers for example cannot distinguish between plastic, protein, and degraded polysorbate which are all very similar in morphology. Technologies available for detailed chemical composition ID such



as Raman microscopy/spectroscopy have been used to fill in the gaps left by particle counters; however, they are tedious, require lots of expertise and extensive signal processing, and have the throughput of a single particle per several minutes of use, making the technique useful only to expert users during failure mode analysis.

In order to fully characterize particulates and aggregates in biopharmaceutical product formulations, further information about the identity of all the particulates is crucial. Regulatory agencies expect drug manufacturers to move away from simple counting techniques and apply multiple and orthogonal methods to complement compendial methods.

In this application note we introduce Fluorescence Membrane Microscopy (FMM). FMM, exclusively available in the Aura® system, is a high throughput, low volume, subvisible particle identification technology. FMM enables ultra-fast, 100% sampling efficiency, characterizing all particles from a single protein aggregate to tens of millions of particles in an entire multi-sample formulation, in under two hours for 96 samples.

Fluorescence Membrane Microscopy

Fluorescence membrane microscopy (FMM) is a novel particle identification method that builds on Backgrounded Membrane Imaging (BMI) to identify, categorize, and further scrutinize the most common particles in an entire bioformulation sample by using established extrinsic fluorescent dye chemistries.

BMI, the backbone analysis technology used in the Aura and Horizon® instruments, images a 96-well membrane plate before and after sample filtration, and conducts novel, high optical contrast image

analysis to resolve particles from 1 µm to 5 mm in size, with a large >36/mL counts dynamic range. Using fluorescent dyes, biopharmaceutical particles are stained and analyzed with FMM to confirm and quantify their presence. To enable FMM, Aura uses new membrane plates specifically manufactured to support labeled fluorescent workflows.

With BMI, the software knows where every particle resides on the membrane, and most importantly all the relevant particle information from counts, sizing, morphology, and light scattering intensity is extracted from what is known as the "particle mask". In FMM, Aura measures the fluorescence signatures only were a particle has first been detected and measured (sized and counted) using BMI, using the fluorescence information for chemical identification only as shown in Figure 1 below. Particles that exhibit fluorescence significantly above the dark fluorescent background from the membrane plates, can then be specifically identified as protein, as is elaborated below.

FMM Workflows

There are two main particle fluorescent staining approaches in FMM:

1 Solution Phase Staining: labeling the particles in solution

Most traditional fluorescence experiments are conducted in solution. However, this approach presents important drawbacks from a particle analysis standpoint: labeling the particles in solution dilutes the sample and introduces buffer and dye chemistries that may impact the sample's chemical properties and stability. Solution staining chemistries can be very invasive, particularly if the matrix solution is



nonpolar. In addition, fluorescent incubation times can be prohibitively long and limit real time use.

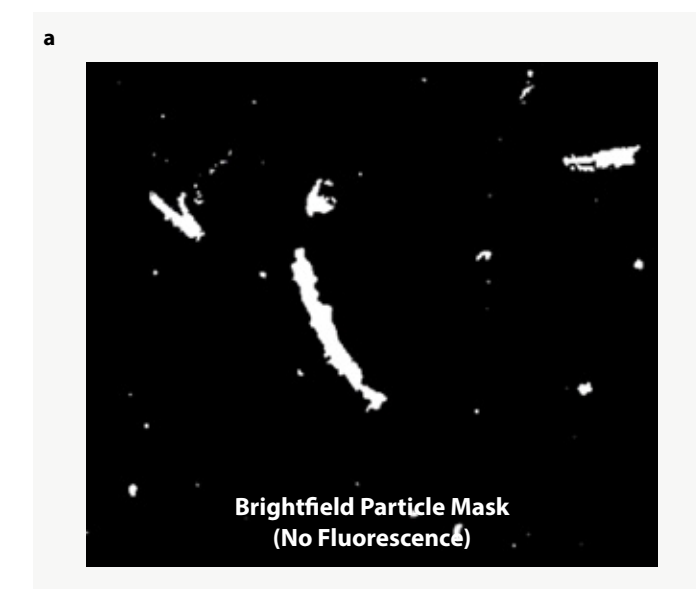
2 Membrane Phase Staining: labeling the filtered particles on the membrane

Membrane Phase Staining is the fluorescent labeling of particles previously captured on the membrane surface. Applying a fluorescent label after sample filtration has many advantages. FMM can be run on particles previously measured on the membrane with BMI, which is a well-established particle measurement method that builds from USP 788 Membrane Microscopy Method 2. This allows FMM fluorescent analysis to be conducted only on "real particles" measured in brightfield, completely decoupling the impact of the fluorescent chemistry from the brightfield particle detection where the true sizing and counting of the particles is done. This allows one to conduct traditional BMI analysis,

and if the user wants to ask additional questions of the particle or sample's composition, FMM can be used. This workflow is shown in Figure 2.

Steps 1 through 3 in the workflow are the same steps as BMI where all the particle counting and sizing takes place. The fluorescent dye is then processed as shown in Step 4, after which the user reinserts the plate back into the Aura instrument for fluorescence measurement and analysis.

There are several ways in which FMM can be conducted, including hybrid methods were some of the samples can be processed using solution phase staining and others using membrane phase staining. In the case studies below, we show two different ways of conducting Membrane Phase Staining. Importantly, the user does not need to pre-specify how FMM will be conducted since the software is designed to automatically align all the fluorescent images with the corresponding brightfield images for accurate analysis.



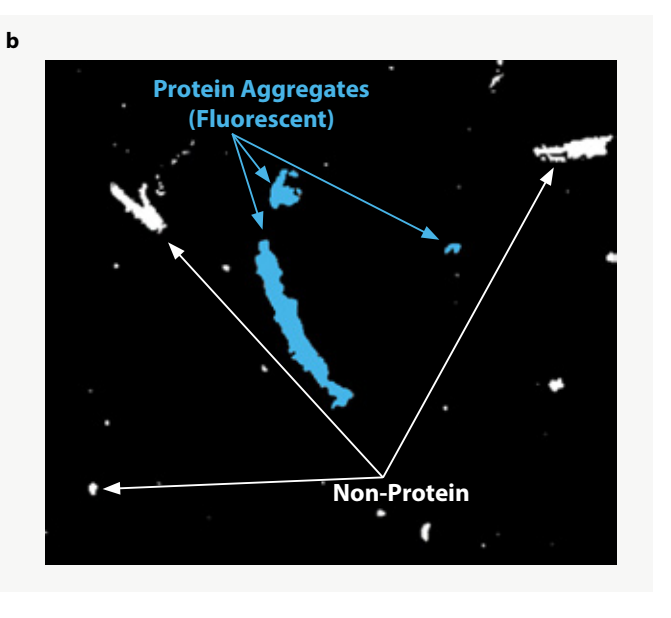


FIGURE 1: The Particle Mask and FMM: (a) Brightfield particle mask characterizes entire particle distribution (size and counts). Black region denotes no particles measured; white regions denotes measured particles in BMI. (b) FMM conducted after fluorescently labeling proteinaceous particles in a protein/non-protein mix.



FMM Identifies Protein Particles Labeled Using Thioflavin T

One of the most important questions in particle analysis is if a given particle or group of particles in a sample is mostly proteinaceous (the drug product) or whether the particles arise from another source. Protein vs. non- protein particle determination marks a critical junction in identifying the main underlying issues with a protein formulation and bypassing this step can result in dramatic missteps and time lost downstream.

To enable protein/non-protein determination, the first fluorescent channel in the Aura system is equipped with optics for specific protein aggregate fluorescent detection using Thioflavin T (ThT) excitation (Ex: 440/40 nm) and emission (Em: 500/40 nm) (Figure 3). Thioflavin T is a widely used, validated dye for protein aggregate

fluorescent labeling and has been used in neurodegenerative disease research like Alzheimer's and Parkinson's for decades³. It specifically binds to amyloid fibrils⁴, misfolded Beta sheet structures that are very common amongst the highly misfolded subvisible protein aggregates. While the mechanism of how ThT binds to these fibrils is beyond the scope of this application note, as multipe mechanisms of binding have proposed⁵, it remains the benchmark for labeling protein aggregates. Its specificity to protein aggregates, high solubility in water, strong fluorescence, well validated body of literature and affordability make it the default protein aggregate staining dye of choice for the Aura system.

Membrane Phase Staining Kinetics

One of the main advantages of membrane phase staining with ThT is rapid staining kinetics. Figure 4

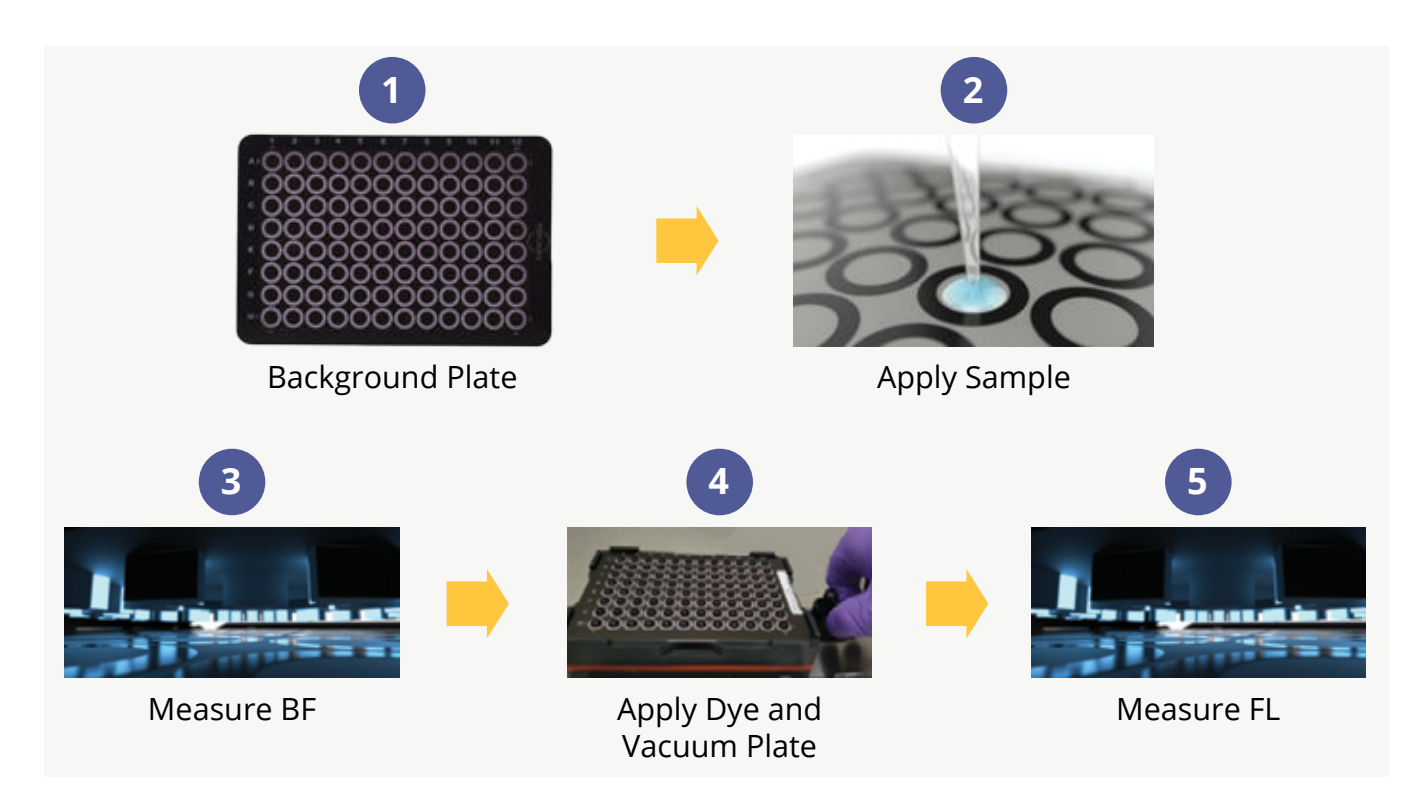


FIGURE 2: FMM Membrane Phase Staining Protocol. Step 1 - Brightfield background. Step 2 - Filter sample. Step 3 - Brightfield measurement. Step 4 - Apply and filter stain. Step 5 - Fluorescence measurement.



shows membrane phase staining of hlgG aggregates that had been previously captured on a membrane. They were then labeled with 50 µL of 5 mM ThT solution in 100% H20, and the dye droplet was vacuumed immediately (Figure 4a) and after 3 minutes of resting on the membrane (Figure 4b). There was no measurable difference in staining efficiency between these two on-membrane incubation times. The fast staining kinetics likely results from all the particle filtrate being highly localized onto a single surface on the membrane.

Case Study: Distinguishing the Undistinguishable to Differentiate Between hIgG Protein Aggregates and **ETFE With FMM**

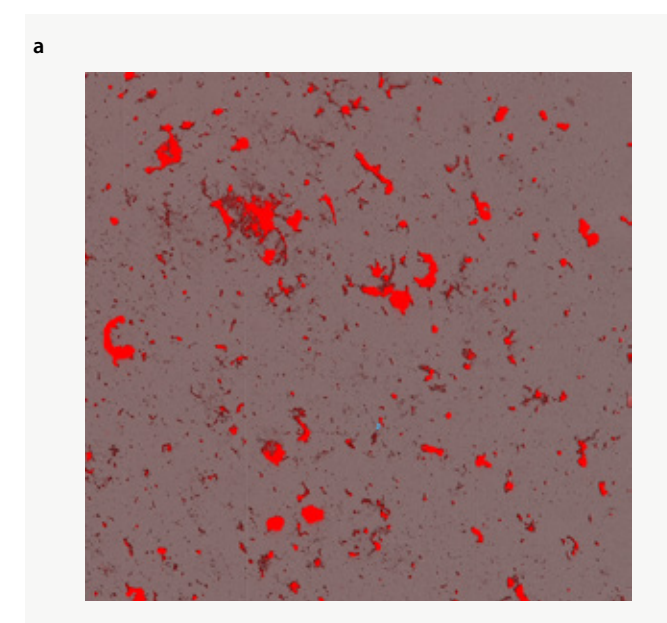
Given the difficulty in characterizing protein aggregates, the National Institutes of Standards and Technology created a protein aggregate mimic from plastic Ethylene Tetrafluoroethylene (ETFE), Reference Material 8634, designed to mimic the morphology, particle distribution, and optical

FIGURE 3: Thioflavin T Molecule.

properties of common aggregated proteins. Many studies, including a detailed one by the Japanese Pharmacopeia⁶, have found that ETFE and protein aggregates are morphologically and optically indistinguishable using Flow Imaging (Figure 5), concluding that simple image analysis and morphology are not enough for absolute protein identity determination.

Experimental Layout

In this experiment we measure hIgG particles generated using rotational stress, ETFE particles from RM8634, and sample mixes consisting of hlgG and ETFE particles. The plate was laid out as shown in Figure 6.



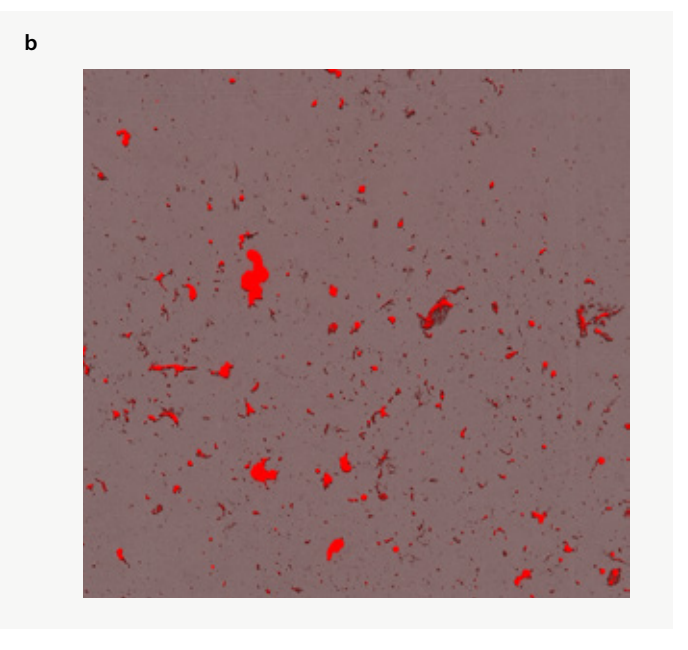


FIGURE 4: Fast staining kinetics on membrane: (a): Fluorescent hlgG aggregates (red) stained with 5 mM ThT which is immediately vacuumed, blotted and read in FMM (b) Fluorescent hIgG aggregates (red) stained with 5 mM ThT after 3 minute on-membrane incubation.



BMI Analysis of hlgG and ETFE

This experiment was conducted using the following sample and volume conditions: 24 wells containing hlgG aggregates, at 50 µL per well, 24 wells of ETFE at 30 µL per well, 24 wells of serially filtrated mixes of hlgG and ETFE (30 µL of ETFE is filtered first, followed by 50 µL of ETFE on the same wells) and 8 wells of water for injection (WFI) controls at 50 µL each. These serial mixes enable controlled experiments as we know how much protein and non-protein particles to expect in the mixed sample, which was generated from unmixed controls with known particle counts. We can later use these count results and compare them with our FMM based protein/non-protein determination which does not use a-priori knowledge of how these particles were mixed.

As shown in **Figure 7**, counts/mL $\geq 2 \mu m$ for each particle measured 49,669 for ETFE, 142,298 for hlgG and 183,997 for the serial lgG + ETFE mix respectively. With the hlgG+ ETFE particle counting

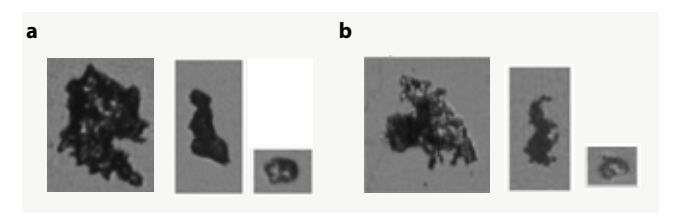


FIGURE 5: Brightfield imaging pictures of (a) protein aggregates are indistinguishable from (b) plastic ETFE particles.

standard error measuring 21,748 Counts/mL for particles ≥2 μm, this experiment shows that the serial filtration mix resulted as expected: the sum of the average counts of the unmixed wells (191,967 Counts/mL $\geq 2 \mu m$) is well within the error of the counts of the serially mixed wells (183,997 Counts/ mL ≥2 μ m).

Fluorescent Image Analysis

We then labeled the entire plate with 5 mM ThT dissolved in WFI at 40 µL per well. On membrane incubation was applied for 1 minute after the final ThT well was pipetted (Figure 2). After processing the dye and blotting the underside of the plate with filter paper, the plate was reinserted into the Aura instrument and the

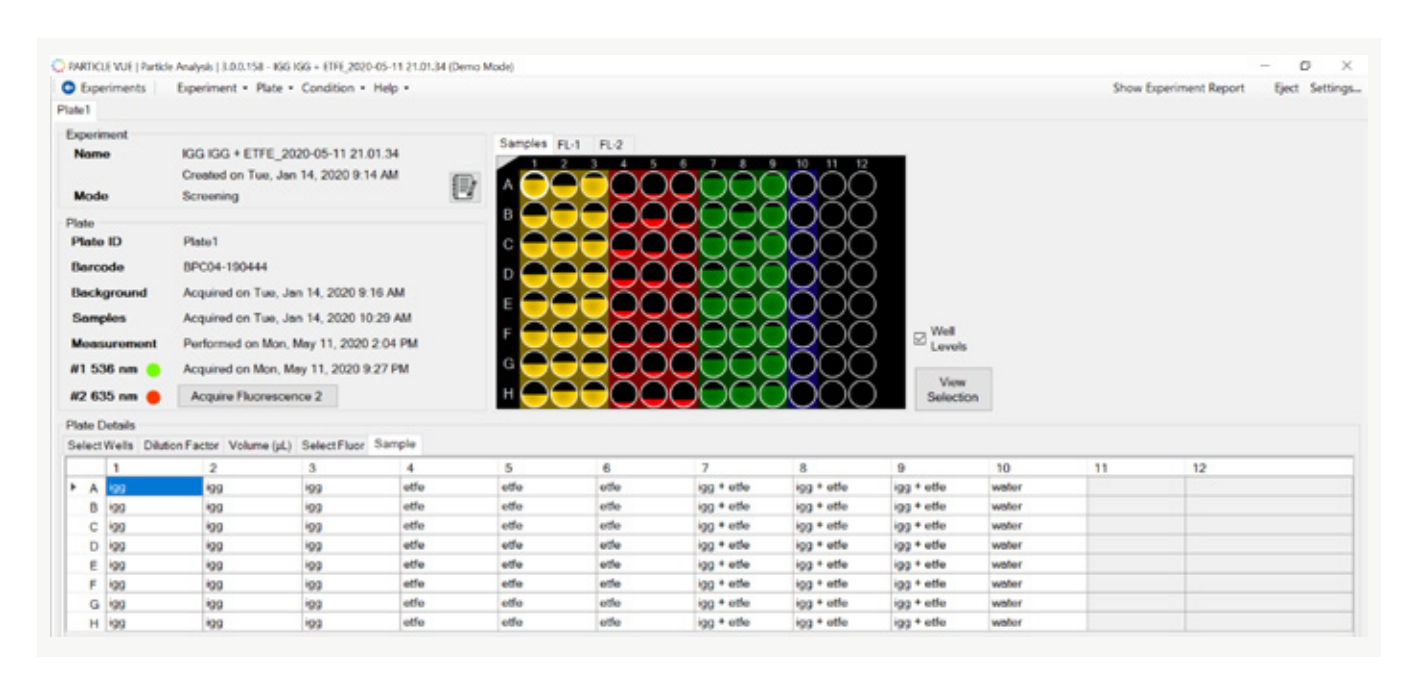


FIGURE 6: Plate layout for Protein/non-protein analysis using FMM of hIgG, ETFE, and mixed hIgG and ETFE particles.



1st Fluorescence Channel data was collected. Figure 8 visualizes wells of each of the protein (hlgG), non-protein (ETFE), and mixed components with ThT Fluorescent excitation (Aura FL Channel 1) and non-fluorescent Side Illumination Membrane Imaging (SIMI).

As seen in Figure 8, there are no particles visible in the WFI control image (Figure 8a) in either fluorescent ThT or SIMI illumination. hlgG particles (Figure 8b) displayed both globular and fibril like morphologies from the rotational stress and exhibited very strong ThT fluorescence (red), due to the binding of ThT to the misfolded beta sheets in these protein aggregates. The hlgG particles did not scatter in SIMI (blue), indicating that these proteinaceous particles do not protrude out of the membrane plane and instead lay flat against it. ETFE particles (Figure 8d) exhibited virtually no ThT fluorescence (or intrinsic fluorescence

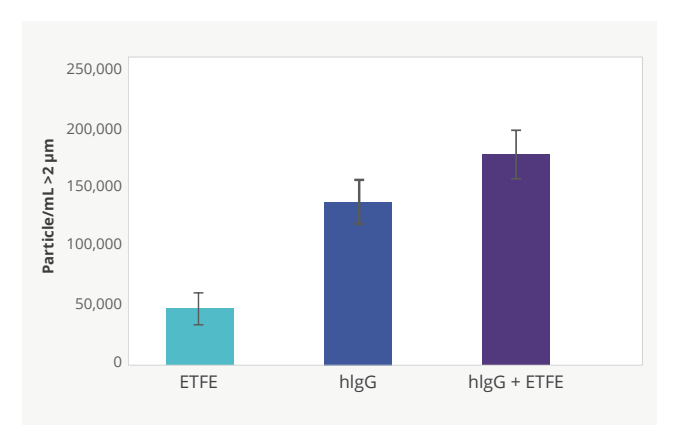


FIGURE 7: Particles/mL ≥2 µm Counts results of ETFE, hlgG, and serial mixes of hlgG + ETFE.

for that matter), however scattered very strongly in SIMI (blue) indicating that these plastic particles protrude out of plane unlike the protein aggregate counterparts. Figure 8c displays an hIgG and ETFE mixed well where both the strong ThT fluorescence signature from the hlgG particles (red) and the strong SIMI scattering (blue) from the ETFE particles can be appreciated simultaneously.

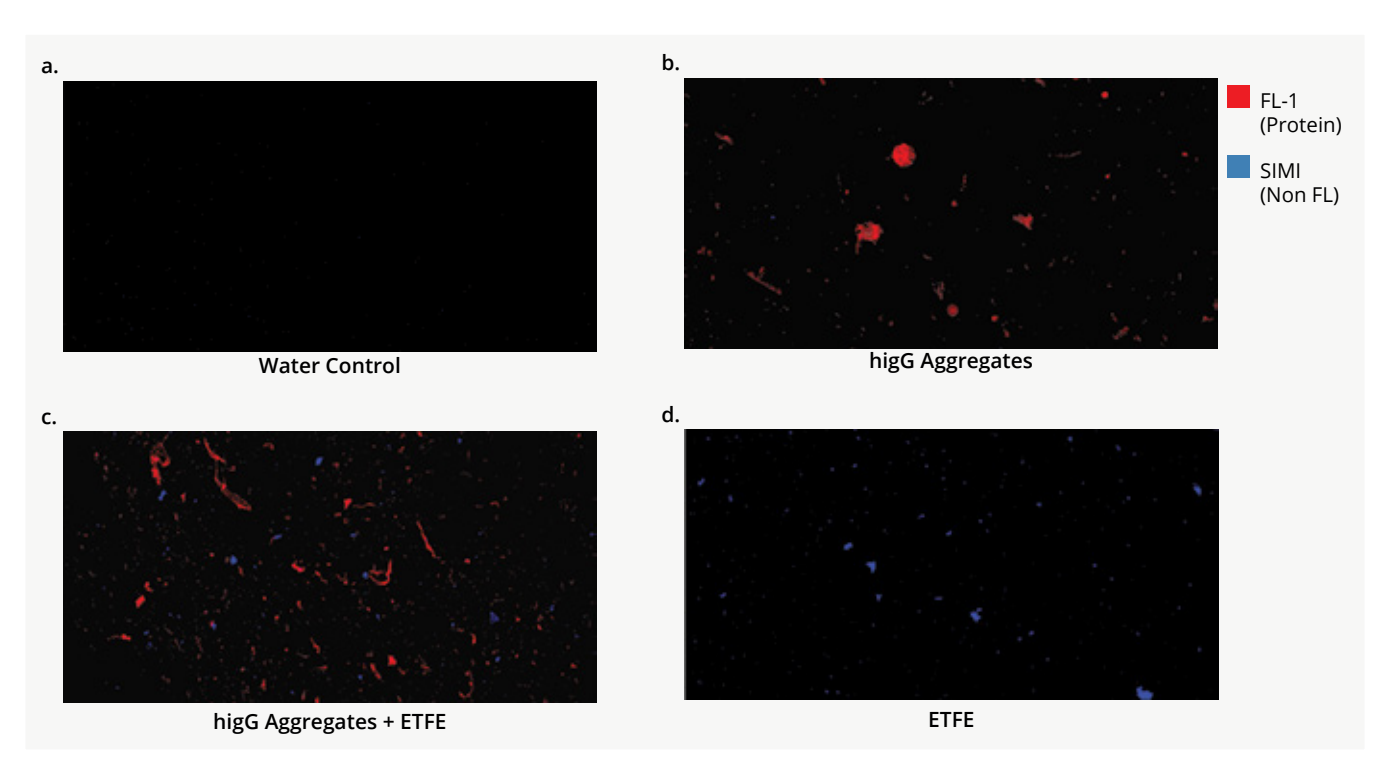


FIGURE 8: Alpha Blended ThT fluorescence (red) and non-fluorescent Side Illumination (blue) images of (a) WFI control (b) hlgG aggregates (c) serial mix of hlgG aggregates and ETFE and (d) ETFE particles.



Whole Well Data Visualization of Proteinaceous and Non-proteinaceous Particles

Figure 9 displays particle scatter plots showing normalized average ThT Fluorescence Intensity vs. Equivalent Circular Diameter Size (µm) for every particle in 3 distinct, ThT labeled wells: hlgG aggregates (a), ETFE (b) and hIgG + ETFE mixtures (d), where each dot represents a single measured particle. Figure 9a shows how labeled hlgG aggregates fluoresce in proportion to their size due to the presence of more binding sites in larger particles. Most importantly, all hIgG particles display fluorescence above the background (the 0 mark). ETFE particles in Figure 9b do not fluoresce (all dots close to the 0 FL background), indicating that ThT did not bind to ETFE. Figure 9c shows a scatter plot of a well containing a mixture of ETFE particles and

hlgG aggregates. This figure shows that the mixed sample exhibit the aggregate properties of the unmixed samples—strong fluorescence from the hlgG particles, and a subpopulation that displays almost no fluorescence (ETFE).

More broadly, scatter plot data visualization can be easily configured in Particle Vue software to aggregate data from select wells while plotting any particle attribute against another. Using the same selected wells from Figure 9, this 3 well data was collapsed into a single scatterplot. In Figure 10, we show Average Normalized Channel 1 Fluorescence vs. Average SIMI Intensity for every particle of these 3 wells. This figure corroborates that there are two very distinct particle populations: One that fluoresces under ThT labeling and excitation that

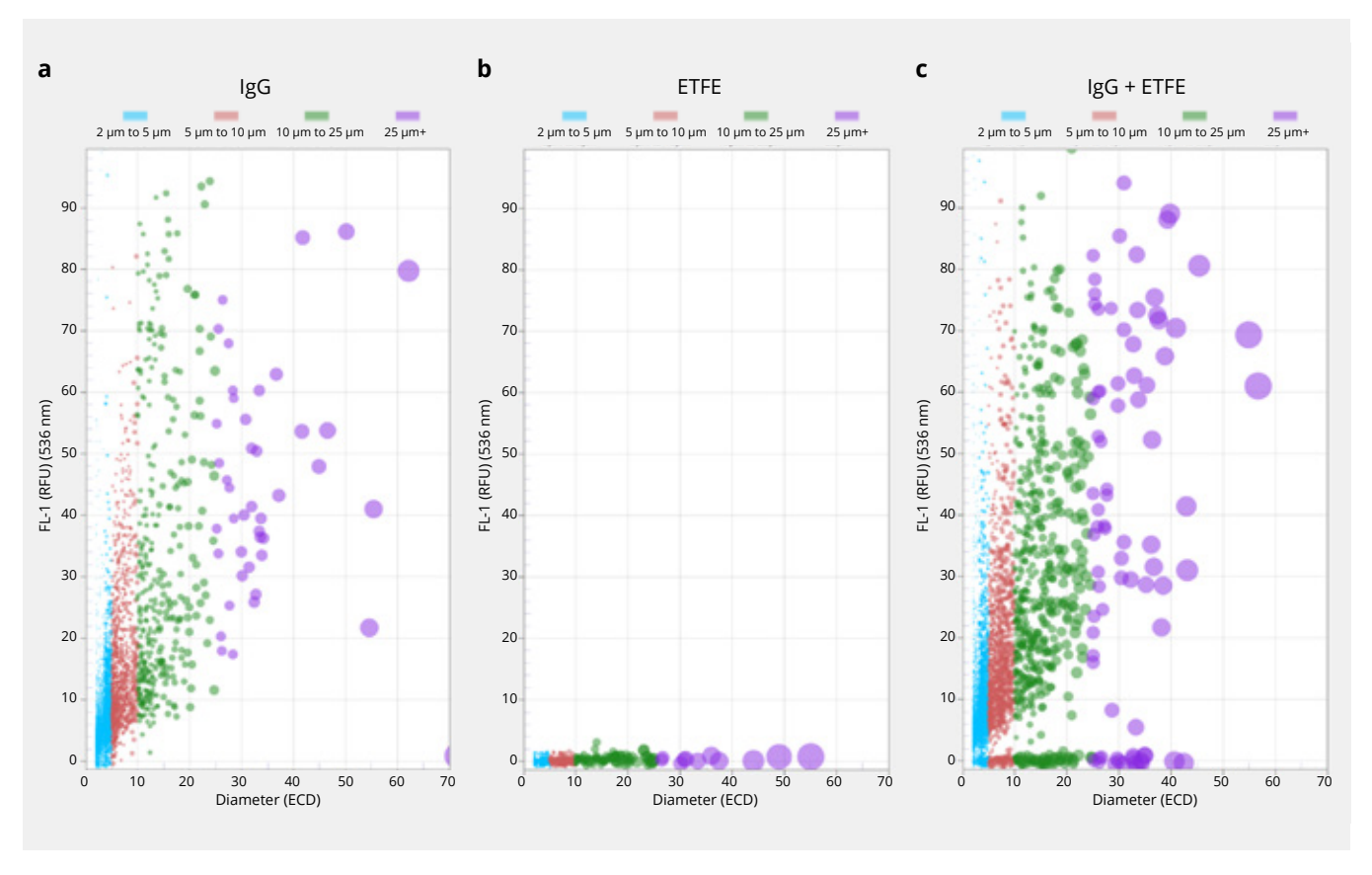


FIGURE 9: Normalized ThT Fluorescence vs. Equivalent Circular Diameter (µm) for labeled (a) hlgG aggregates (b) ETFE and (c) hlgG + ETFE particle mixtures.



does not protrude out of plane (no SIMI), while another population does not fluoresce after ThT labeling, but protrudes significantly out of plane, just as seen visually in Figure 8. In other words, hlgG aggregates and ETFE particles could not be any more different! Using FMM in the Aura system, we were able to distinguish them using specific fluorescence and unique geometry (SIMI), which is not possible with flow imaging.

Analysis of Mixed Particles

While most of the particles in the serially mixed solution clearly showed separate subpopulations, some large particles showed intermediate SIMI and fluorescence intensities, indicating that they might have both protein and non-protein components. One such mixed particle is shown in Figure 11. Figure 11a shows the brightfield difference image for this particle, Figure 11b the SIMI intensity

image, Figure 11c the fluorescent image, and Figure 11d the combined SIMI and Fluorescence alpha blended image. Out of plane features (strong SIMI) are characteristic of the left-hand side of the particle (ETFE), and ThT fluorescence on its righthand side (hlgG aggregate portion), while the particles around it show unmixed characteristics.

FMM Statistical Analysis for Protein/ Non-Protein Determination for the Entire **Experiment**

Particle Vue software also allows total statistical analysis for protein/non-protein determination from a single particle, to a single well to an entire experiment for high level insights. This is done using two methods: (1) Manual Threshold analysis and (2) Expression Engine based analysis. While both methods are implemented differently, they are both based on establishing a fluorescence

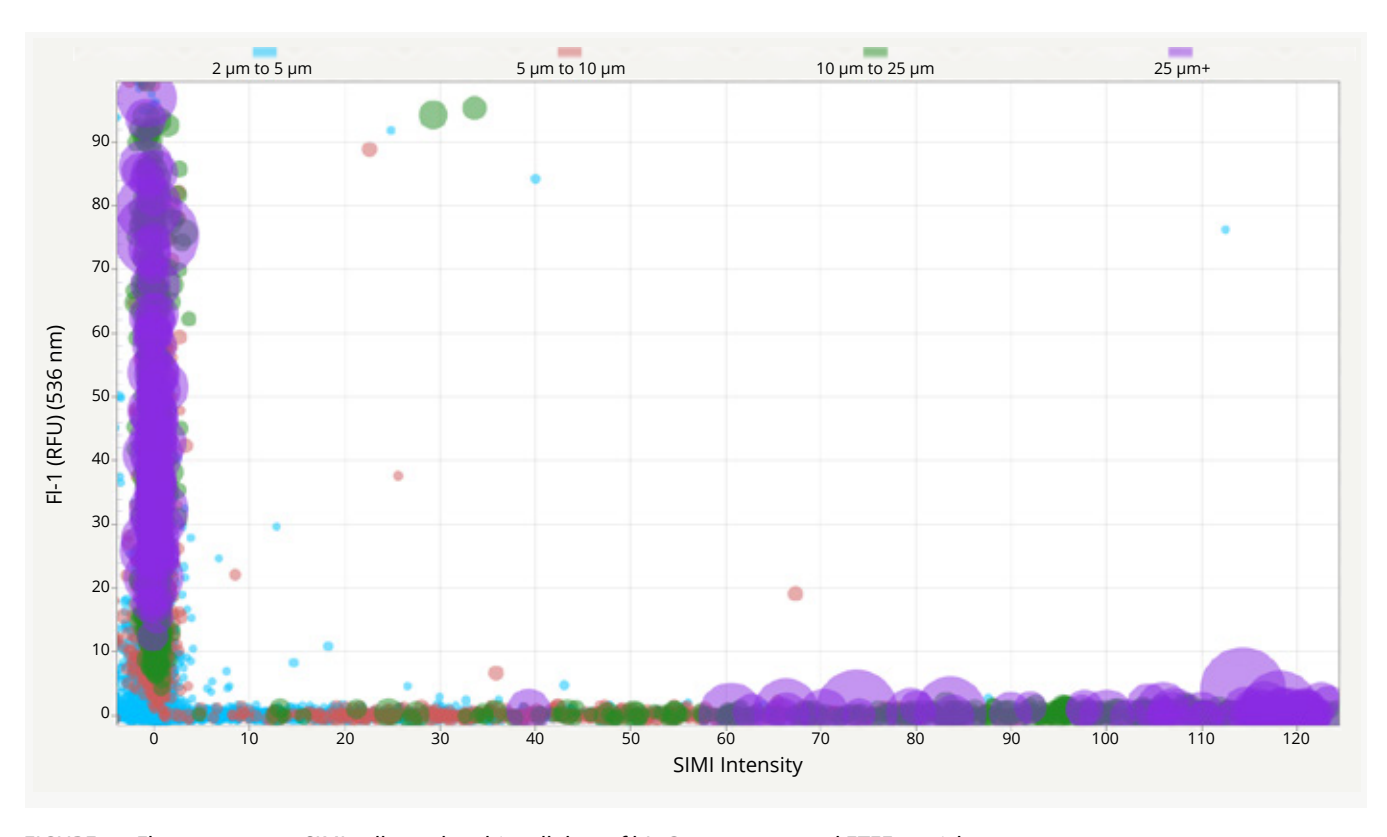


FIGURE 10: Fluorescence vs. SIMI collapsed multi-well data of hlgG aggregates and ETFE particles.

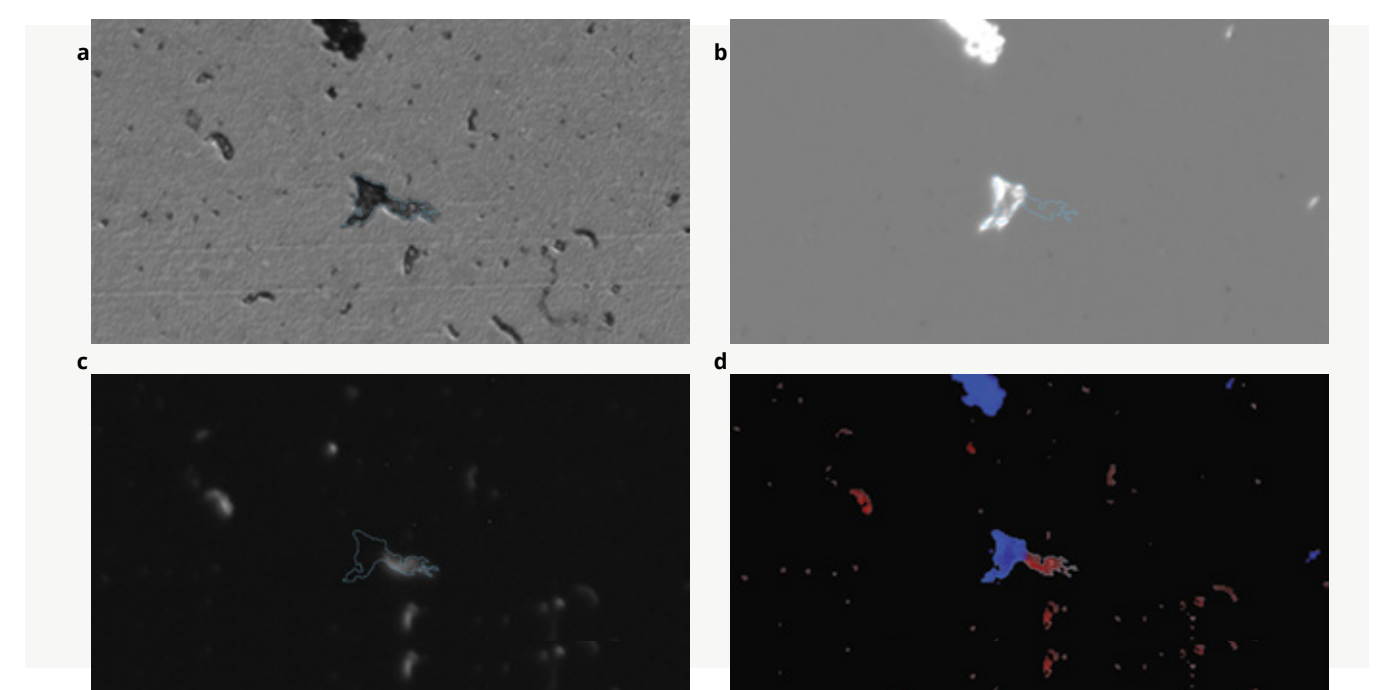


FIGURE 11: A mixed ETFE and hlgG particle imaged via (a) Brightfield difference (b) SIMI intensity (c) Fluorescence intensity signature and (d) Combined SIMI and Fluorescence alpha blended image.

intensity baseline (threshold) for which a particle above this baseline will be considered labeled (in the case of ThT fluorescence—a protein aggregate) or below it and therefore not labeled (not a protein aggregate).

Manual Thresholding

Using the Manual Threshold option in the scatterplot, the data can be split into four separate quadrants. This is done by manually selecting an x-axis threshold and a y-axis threshold, both denoted with dotted lines in Figure 12. In this case, the data was split by ECD >5 µm in the x-axis and normalized fluorescent threshold intensity of 3—an intensity well above the background fluorescence exhibited by the membrane and the non-fluorescent ETFE particles, in the y-axis. These thresholds were then locked in the software (locking the axis for comparison as well as the thresholds), which then split the particle data into four quadrants as shown in Figure 12. For threshold data locked as shown, Quadrant 2 contains

all particles above 5 µm in size that exhibit strong ThT fluorescence. Particles below the horizontal threshold exhibited almost no ThT fluorescence and are likely to not be a protein particle. With the thresholds now locked, the manual threshold cumulative table outputs the data below in Table 1.

Some quick insights can be gained with the manual threshold approach: ETFE has almost no particles in Q1 and Q2, the high fluorescent quadrants, and most of its particles reside in the Q3 and Q4. For hlgG aggregates, most of its particles are in the top two Quadrants where fluorescence is well above the fluorescence baseline. For a more specific and in-depth analysis, the Expression Engine is used as shown in the next section.

Sample	Replicates	%CV ≥2 μm	Q1	Q2	Q3	Q4
ETFE	24	26.35	192	254	32302	17022
IgG	24	13.28	78470	48681	15123	146
IgG + ETFE	24	11.82	89000	64358	22040	8921

TABLE 1: Threshold quadrants for ETFE, hIgG and mixed particles.



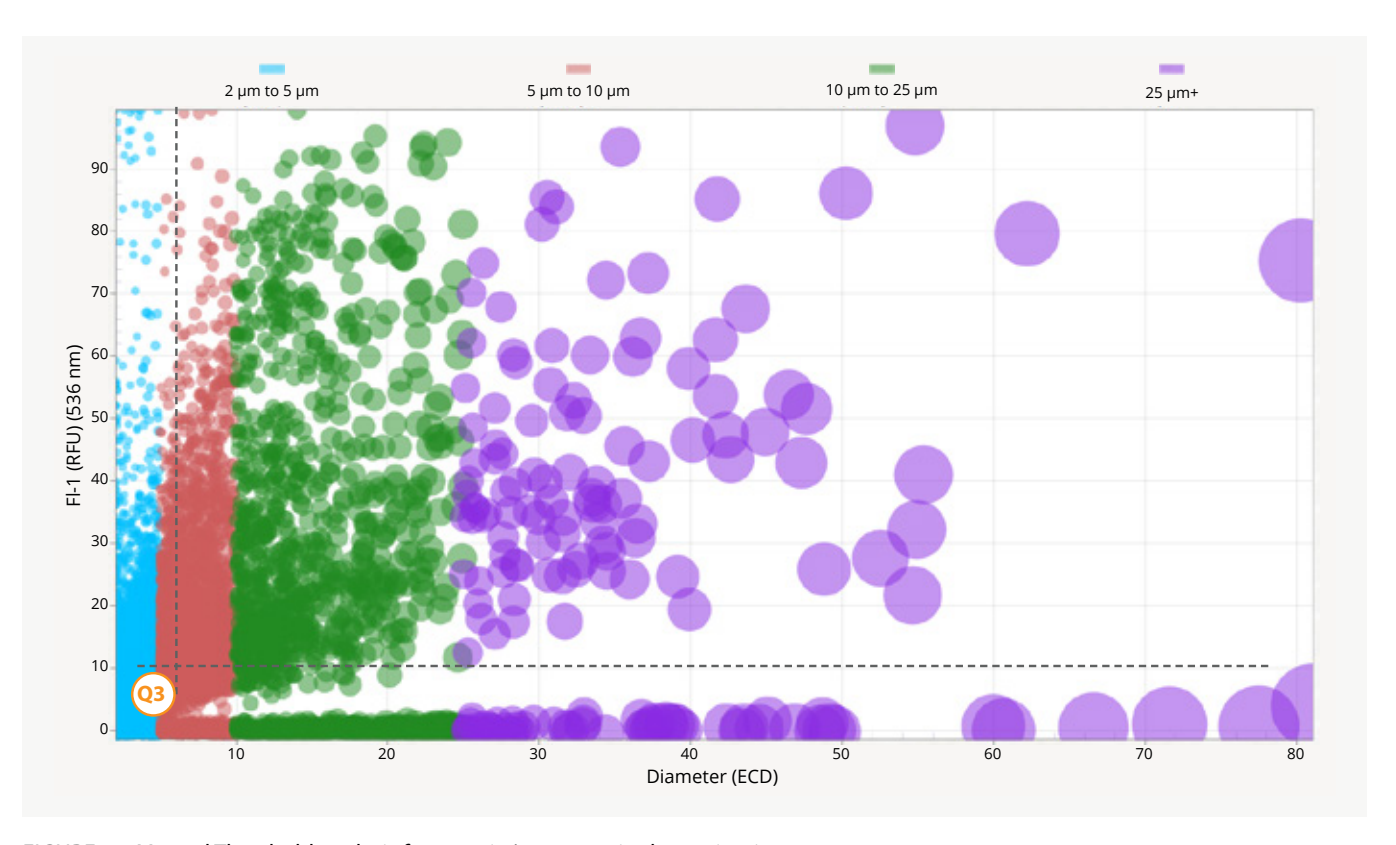


FIGURE 12: Manual Threshold analysis for protein/non-protein determination.

Expression Engine Based FMM Analysis

One of the most powerful features of the Particle Vue software is the Expression Engine. Every particle attribute: size, morphology, SIMI and fluorescence scattering intensity, etc., is stored for every single particle in the software as shown in Figure 13. The expression engine allows one to leverage this wealth of data by guerying for particles that meet desired criteria. This is done by selecting the desired particle properties from a selection table and apply Boolean logic tests to characterize the population.

For example, the expression text in Figure 13 interrogates how many particles ≥2 µm in Equivalent Circular Diameter show an average fluorescent intensity in the first channel (ThT labeled fluorescence), which is 6 standard deviations above the membrane background fluorescence. If it meets the criteria, the user can be confident that the

particle is proteinaceous in nature. To use the expression engine in more detail, the results from **Table 2** below were obtained by creating 4 simple expressions:

- 1 Expression: Diameter >2—Returns how many particles >2 µm are present for every sample
- 2 Expression: FL1Intensity>FL1Background+6* FL1Background and Diameter >2—Returns how many protein Particles >2 μm are stained by ThT and are considered proteinaceous
- 3 Expression: Diameter >5—Returns how many particles above >5 µm are present for every sample
- 4 Expression: FL1Intensity>FL1Background+6* FL1Background and Diameter >5—Returns how many protein Particles >5 μm are stained by ThT and are considered proteinaceous



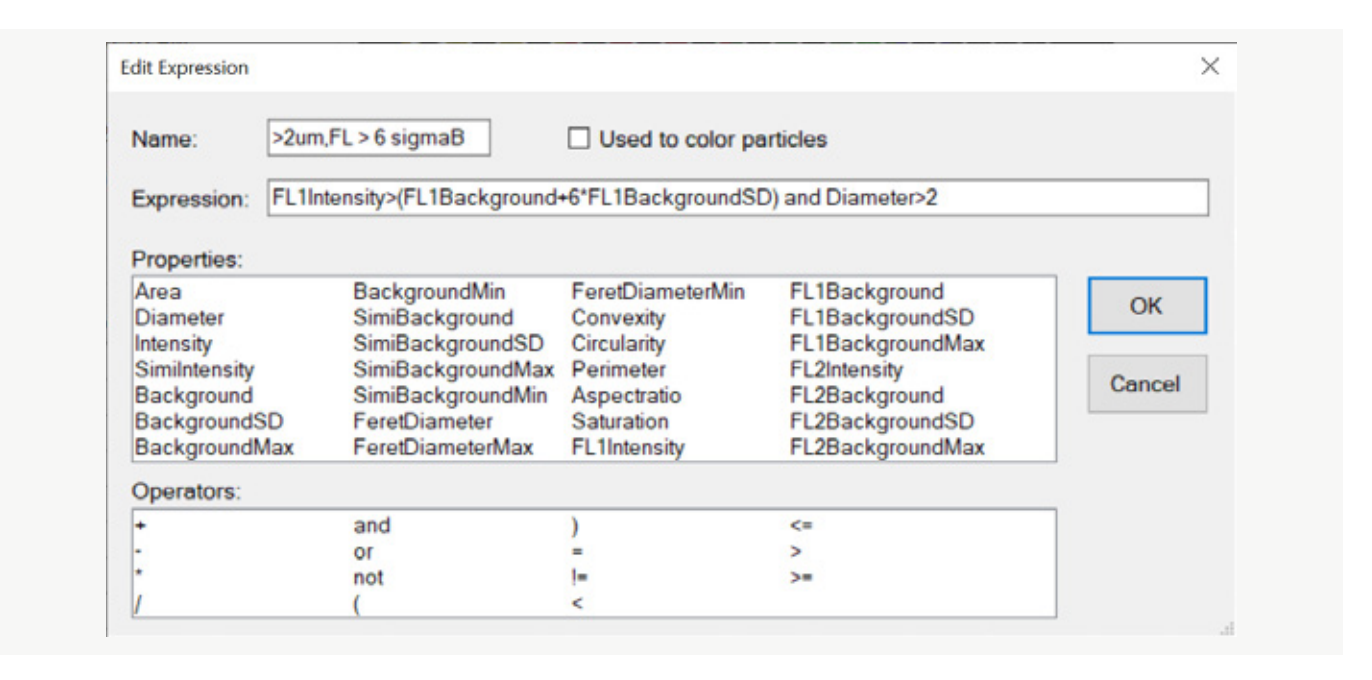


FIGURE 13: Particle Vue Expression Engine.

Table 2 summarizes the total counts for each particle type, the fluorescent counts above the background, and the percentage of the fluorescent (protein) counts of the overall population, which were directly outputted by the expression engine. ETFE particles were only mischaracterized as proteinaceous 0.9% of the time for particles ≥2 µm and only 1.5% of the time for particles ≥5 μm, a very low false positive rate. hlgG aggregates, on the other hand, were identified 90% of the time for ≥2 µm and virtually 100% for particles ≥5 µm. The presence of more binding sites (misfolded Beta sheets) in the larger aggregates likely accounts for the increased ThT fluorescence staining efficiency.

As shown in **Table 2**, the serial mixes of hlgG aggregates with ETFE displayed an 83.5% and 87.8% total protein component for particles for ≥2 µm and ≥5 µm respectively. Because this experiment was controlled, we know how much protein and non-protein particle material there was to begin with. That means we can compare the ratio of ETFE/Mix from a particle counts standpoint and compare these results to our counts obtained via FMM analysis. In Table 3, we show that FMM did accurately predict the proteinaceous component of the mixture. The non-protein counts predicted by FMM is identical to the expected controlled counts experiment for particles above $>2 \mu m$ and $>5 \mu m$.

Sample	Replicates	ECD >2 μm (/mL)	"Protein">2 μm (/mL)	%"Protein" >2 μm (/mL)	ECD >5 μm (/mL)	"Protein">5 μm	%"Protein" >5 μm (/mL)
ETFE	24	49768	467	0.9%	15857	244	1.5%
hlgG	24	142419	127865	89.8%	43494	43396	99.8%
hlgG + ETFE	24	184318	153492	83.3%	66343	58223	87.8%

TABLE 2: Summary of particle counts, fluorescent counts and % protein obtained using the Expression Engine.



ETFE amount in mix	>2 µm	>5 µm	
Calculated by Counts	15.5%	14%	
Calculated by Fluorescence Thresholding	15.5%	12.2%	

TABLE 3: Non-protein component in mixed protein/non-protein population.

We then subjected several non-proteins to ThT FMM. Different wells containing Palmitic Acid particles (polysorbate degradation fatty acid constituents) (Figures 14a), Corning® Cryovial Particles (Figures 14b), and Stainless-Steel Particles (Figure 14c) were all stained with 40 µL of 5 mM ThT each and measured via the Membrane Phase Staining method shown in Figure 2. Corning cryovial delaminated particles can be easily formed by vortexing any solution in a Corning Cryovial for 1 minute, resulting in counts exceeding 30 k/mL above 2 µm. The fluorescence staining efficiency in ThT for particles >5 μm

were below <5% for all these non-protein control particles, which can also be appreciated from the dark fluorescence images. This shows that common non-protein particles in protein formulations like plastics, polysorbates and metal have low to no cross staining with Thioflavin T, making this assay specific to protein identification.

Conclusion

FMM using ThT allows one to conduct high throughput, low volume and specific protein/ non-protein particle analysis. The power of FMM using ThT is the ability to obtain protein/

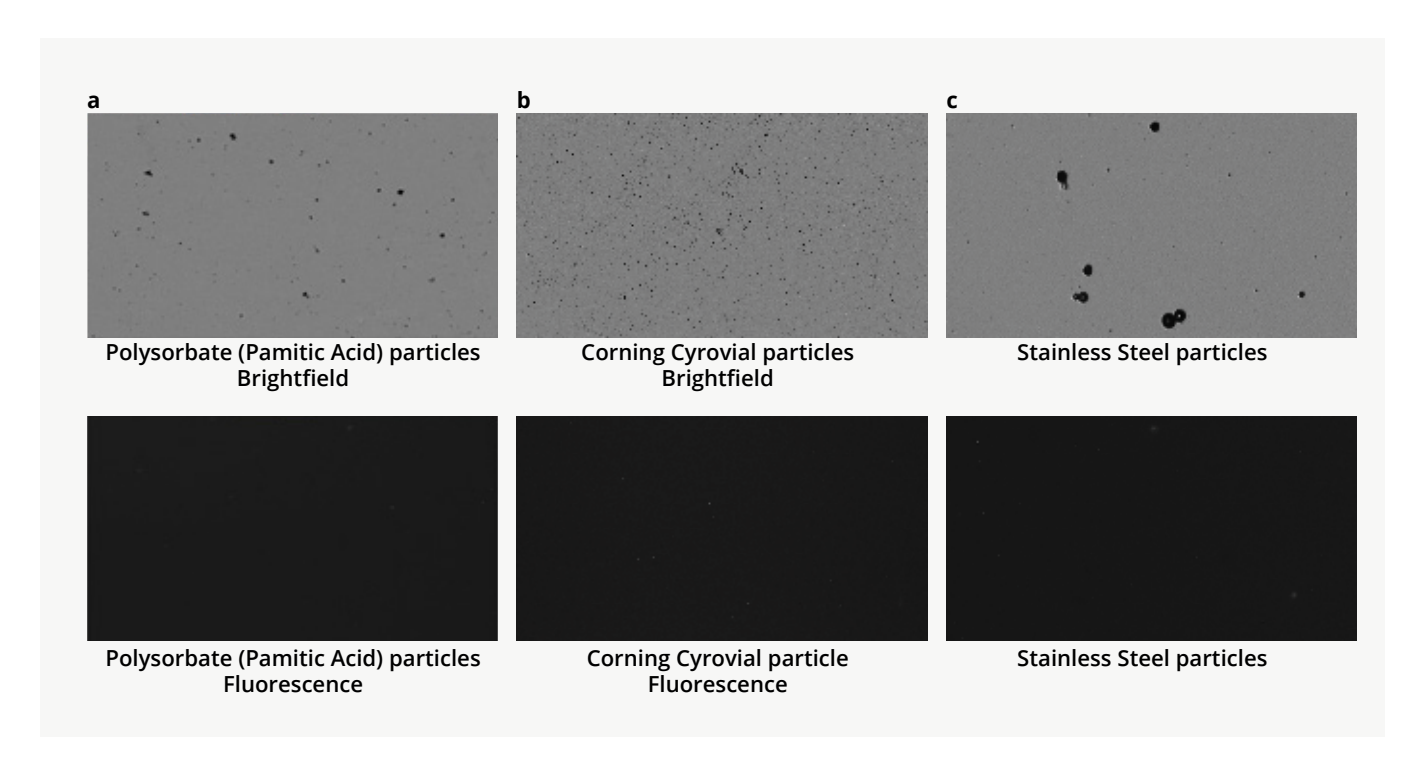


FIGURE 14: Negative Control: Non-proteins imaged in brightfield (BF) and 5 mM ThT stained fluorescence images (FL) modes: (a) BF difference image of palmitic acid particles (top) and FL image of palmitic acid particles (bottom). (b) BF difference image of Corning cryovial plastic delaminated particles (top) and FL image of Corning cryovial plastic delaminated particles (bottom). (c) BF difference image of 20 µm stainless steel particles (top) and FL image of 20 µm stainless steel (bottom).



non-protein ID for a whole 96-well plate assay down to a single individual particle in less than 90 minutes. ThT's high solubility and specificity to protein aggregates makes it possible to differentiate protein aggregates from particles with similar morphology and refractive index like plastics and

fatty acids. Compared to spectroscopic techniques, the throughput of FMM is 1000x higher, while using best in class particle sizing and counting analysis that has its roots in the wellestablished membrane microscopy found in USP 788.

References

- 1. Guidance for Industry Immunogenicity Assessment for Therapeutic Protein Products. US FDA 2014.
- 2. Industry Perspective on the Medical Risk of Visible Particles in Injectable Drug Products. Parenteral Drug Association. 2014.
- 3. Naiki H, Higuchi K, Hosokawa M, and Takeda T. Fluorometric determination of amyloid fibrils in vitro using the fluorescent dye Thioflavine T. Anal. Biochem. 1989; 177:244-249.
- 4. Levine III H. Thioflavin T interaction with synthetic Alzheimers's disease β-amyloid peptides: Detection of amyloid aggregation in solution. Prot. Sci. 1993; 2:404-410.
- 5. Groenning M, Olsen L, van de Weert M, Flink JM, Frokjaer S, Jørgensen FS. Study of the binding of Thioflavin T to β -sheet-rich and non- β -sheetrich cavities. J. Struct. Biol. 2007; 158:358-369.
- 6. Kiyoshi M, Shibata H, Harazono A, Torisu T, Maruno T, Akimaru M, Asano Y, Hirokawa M, Ikemoto K, Itakura Y, Iwura T. Collaborative Study for Analysis of Subvisible Particles Using Flow Imaging and Light Obscuration: Experiences in Japanese Biopharmaceutical Consortium. J. Pharm Sci. 2019; 108(2) 832-841.





Direct, Non-Destructive Analysis of Subvisible Particles



Scientists have begun testing a new, non-destructive subvisible particle technique whereby subvisible particles of protein, plastic, glass, metal, dust, protein, surfactant degradation, and silicon oil droplets, for example, can be detected effectively in potential drug products, even among filled product. Additional benefits of non-destructive subvisible particle testing include improved data quality and reduced resource burden.

BY GAIL DUTTON

he ability to analyze products directly and non-destructively offers a distinct advantage to biopharmaceutical manufacturers. The presence of subvisible particles poses a safety risk for patients, yet manufacturers have grappled for years with ways to efficiently identify, and then remove, them from cell therapies and other parenteral solutions.

Several possible analytical approaches have been proposed in the past few years, such as backgrounded membrane imaging, which may be effective with working with limited sample material, and imaging flow cytometry, which was suggested as providing supportive data but not for routine use for quality control.

"Analysis systems based on the two leading methods—light obstruction and counting microscopic particles—generally require destruction of the sample material during the measurement



process," Changhuei Yang, PhD, professor of electrical engineering at California Institute of Technology (CalTech), tells GEN.

Yang and colleagues at Amgen and CalTech may have a solution. Writing in the Journal of Pharmaceutical Sciences, they detail their work to develop a direct, non-destructive analyzer that determines whether subvisible particles are present in injectable and ophthalmic solutions. Notably, their approach analyzes subvisible particles in their containers, thereby avoiding the need to remove [and hence destroy] product for testing.

Reducing Distortion

Yang and his team developed a custom sample housing for the analyzer that minimizes optical distortions caused by the curvature of the product vials. During the analysis, the equipment used Mie scattering theory and existing refractive indices to model side scattering from any individual particle.

The scientists then estimated the spherical particle size and particle concentration. "These measurements are performed rapidly and simultaneously for all the particles seen through a light-sheep microscope," Yang says. "As such, the system is also able to generate a size-sorted particle concentration report of the sample."

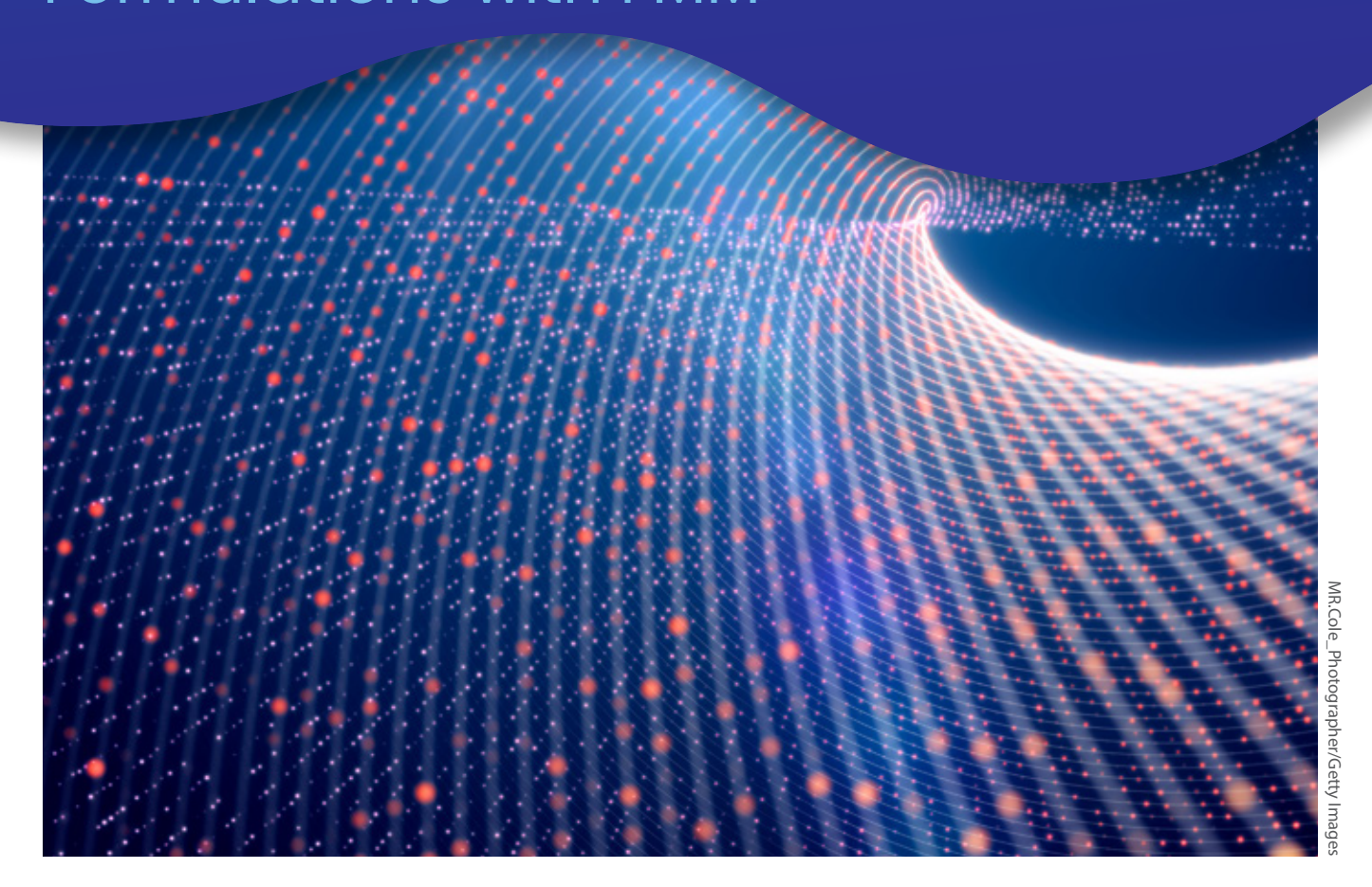
To test the accuracy of this approach, Yang and colleagues evaluated polystyrene bead suspensions in ISO 2R and ISO 6R vials. Results showed the analyzer accurately detected subvisible particles in those containers and sorted them "into commonly used size bins—equal to or greater than 2, 5,10 and 25 microns—and quantified particle concentration between 4.6e2 to 5.0e5 particles/mL."

Consequently, subvisible particles of protein, plastic, glass, metal, dust, protein, surfactant degradation, and silicon oil droplets, for example, can be detected effectively, even among filled product. Additional benefits of non-destructive subvisible particle testing include "improved data quality and reduced resource burden," the scientists note.

Applications include stress testing and stability monitoring of drug products, particularly once they are in their primary containers.

GEN

High-Throughput Detection of Degraded Polysorbate in Biological Formulations with FMM



Introduction

he FDA requires that all biologic formulations be free of visible particles and has defined allowable levels of subvisible particles (SVPs) larger than 10 µm to ensure the potency, efficiency, and safety of these drug.1 While most protein drug particle analysis focuses on particles formed due to formulation instability, SVPs formed through the degradation of formulation excipients must also be considered.

Polysorbates 20 (PS20) and 80 (PS80), best known as Tween-20 and -80, are excipients used in

>70% of marketed parenteral biological drugs to improve product stability and shelf life.² However, when these formulations are stored for long periods of time (>6 months) at low temperatures (4 °C), visible and subvisible particles are formed due to the enzymatic hydrolysis of the polysorbates by host cell proteins (HCPs) such as esterases and lipases.^{3,4} PS20 in particular has been found to be extremely prone to degrading into fatty acid particles.5 Lauric, myristic and palmitic acids are the most common fatty acid

degradation products, and there is a direct correlation between low fatty acid solubility and particle formation in common formulation buffers.3-7 However, high-throughput, sensitive, and specific analysis of polysorbate particles has been difficult due to their complex chemistry and their low concentrations (<<0.5%) in high protein concentration (>100–200 mg/mL) formulation environments, making it a perennial needle in a haystack problem.

In this application note, we introduce the Aura® polysorbate degradation assay, a specific and quantitative assay that in a few hours detects free fatty acid particles (FFAs) formed during polysorbate degradation in 96 samples using anywhere from 5 µL-10 mL of sample. The Aura uses backgrounded membrane imaging (BMI) and fluorescence membrane microscopy (FMM) to count, size and ID particles from 1 µm to 5 mm. Fluorescent labels utilized by FMM are selected based on thier ability to interact with particles of a certain nature, allowing for the generation of key information related to identity of the particles.

Method

BODIPY FL C₁₆ Preparation

- 1 Dissolve 1 mg (1 vial) of BODIPY® FL C₁₆ (ThermoFisher, catalog no. D3821) in 1 mL of DMSO to make "Solution A"
- 2 Mix 200 μL of "Solution A" with 643 μL of DMSO to make "Solution B"
- 3 Mix 20 μL of "Solution B" with 980 μL Accetate buffer (pH 4.8) to make 100 μ M BODIPY FL C₁₆

Solutions

The following solutions were prepared in 50 mM acetate, 150 mM NaCl buffer to simulate different test samples.

- 1 Buffer with 0.04% (w/v) PS20
- 2 Buffer with 0.04% (w/v) PS20 and 2.5 μM human IgG (hlgG)
- 3 Buffer with 0.04% (w/v) PS20 and 3FFA
- 4 Buffer with 0.04% (w/v) PS20 and 2.5 μM human IgG (hlgG) and 3FFA
- 5 Buffer with 150 μM lauric acid
- 6 Buffer with 87.6 μM myristic acid
- **7** Buffer with 31.2 μM palmitic acid

We defined "three free fatty acids" (3FFA) as a supersaturated mixture of lauric, myristic and palmitic acids prepared using a combination of published protocols^{3,4} to mimic their concentration in compendial grade PS20. The mixture contains 56% lauric acid, 32% myristic acid, and 12% palmitic acid. The % values were calculated based on the total fatty acid concentration (269 µM). All fatty acid solutions were stored at 4 °C for 3 weeks to generate particles and were used as a positive control for polysorbate particle formation. Buffers and water for injection (WFI) were all filtered (0.2 µm syringe filter) prior to use.

Aura Configuration

An Aura system with two fluorescence channels was used to perform all experiments described. Fluorescence Channel 2 (FL2: excitation 482/35 and emission 524/24 nm) was used to specifically ID fatty acid particles stained by the phospholipid



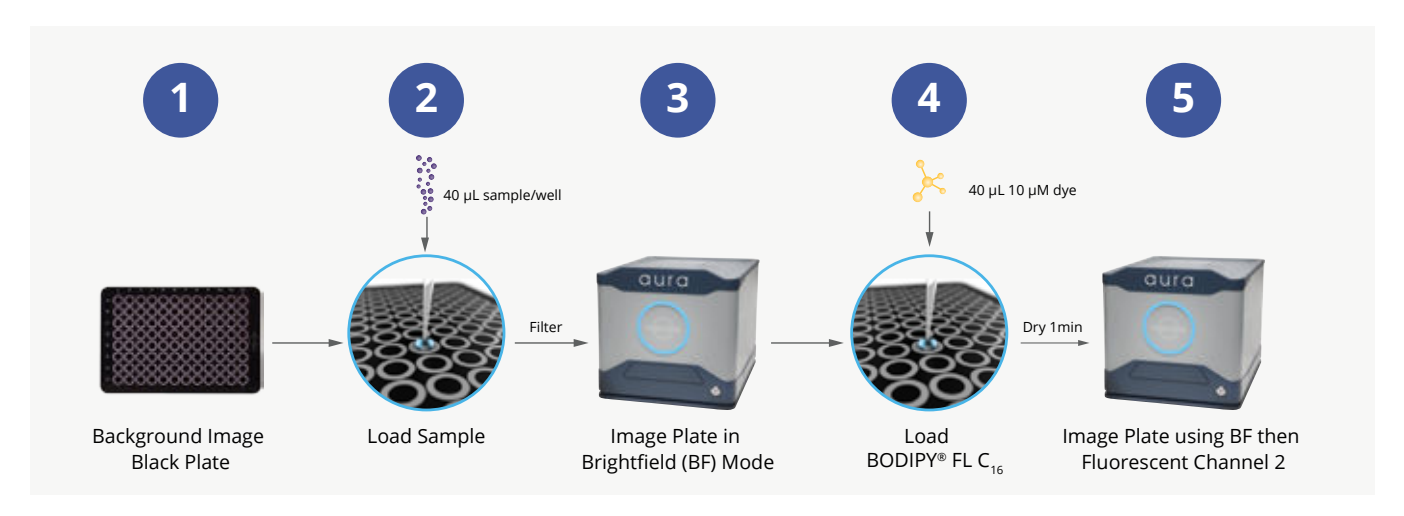


FIGURE 1: The polysorbate degradation assay workflow on the Aura detects degraded excipients, even in high concentration protein formulations. Samples are labeled with Thioflavin-T and BODIPY FL C16 to specifically ID protein aggregates and free fatty acids, respectively, with FMM.

targeting dye BODIPY FL C₁₆. The BODIPY FL C₁₆ was prepared to final concentration of 10 µM in acetate buffer (2% DMSO). We recommend preparing the final staining solution in same buffer as the protein. All sample handling, preparation, and process operations were performed inside a laminar hood.

It is possible to specifically ID protein aggregation and excipient degradation in the same sample. In these situations, label the sample with 5 mM Thioflavin T (ThT) and measure the membrane plate using Fluorescence Channel 1 (FL1: excitation 440/40 and emission 500/40 nm) after labeling the sample with BODIPY FL C₁₆ (See Application Note 7).

Polysorbate Degradation Assay Protocol

To perform the Aura polysorbate degradation assay (Figure 1):

- 1 Background Image a black membrane plate
- 2 Load and filter 40 µL of sample onto the backgrounded plate

- 3 Image the plate in brightfield (BF) mode to count and size all particles in solution
- 4 Label fatty acid particles with 40 μL of 10 μM BODIPY FL C₁₆. Incubate for 1 minute, then filter
- 5 Image the plate first in BF mode, then in FL2 channel

Results and Discussion

Morphological Appearance of Different Fatty Acid Particles

The Aura images every particle, enables subvisible particle size distributions analysis, and makes morphological differentiation possible using built-in image analysis filters. When we analyze different free fatty acid solutions in the Aura, we find that each forms particles with different morphological characteristics. Lauric acid particles are large and irregular clusters, myristic acid particles are small and oval shaped, and palmitic acid particles form fibril-like particles and small circular clusters (Figure 2a-c). These unique morphological characteristics suggest the presence of free fatty acid particles that can then be confirmed with FMM using labeled fluorescence.



Fluorescent Identification of Fatty Acid Particles Using BODIPY FL C₁₆

BODIPY FL C₁₆ is a high affinity stain specific to fatty acid particles. To evaluate its staining efficienty, we measured the percentage of particles of a given population that fluoresce over the dark membrane background. In the combined BF and FL images shown in Figures 3c and 3f, particles that are not stained by BODIPY FL C₁₆ appear grey while the ones that are stained appear green. When the negative control hlgG sample was analyzed, only 28,776 counts/mL of particles of the total 442,600 counts/mL counted using BF fluoresced indicating a BODIPY FL C₁₆ staining efficiency of 6% (Figure 3b, c). However, when the same BODIPY FL C₁₆ staining solution was added to the 3FFAs

sample, where we expect to see particles attributed to excipient degradation (Figure 3d), 73% of the total particles fluoresced strongly and appeared as green (Figure 3e, f). It's also possible to individually identify the 3FFAs particles based on their size, shape, fluorescent intensity and even relative abundance, as demonstrated in Figure 3f. Here, we see that the larger lauric acid particles fluoresce more than myristic particles which in turn fluoresce more than palmitic acid particles when stained by BODIPY FL C₁₆.

Quantitative proof of BODIPY FL C₁₆'s higher selectivity to FFAs over proteins is shown in the Fluorescence vs. Size scatter plots shown in Figure 4. Figure 4a displays how FFA particles of every size fluoresce strongly when stained with BODIPY FL

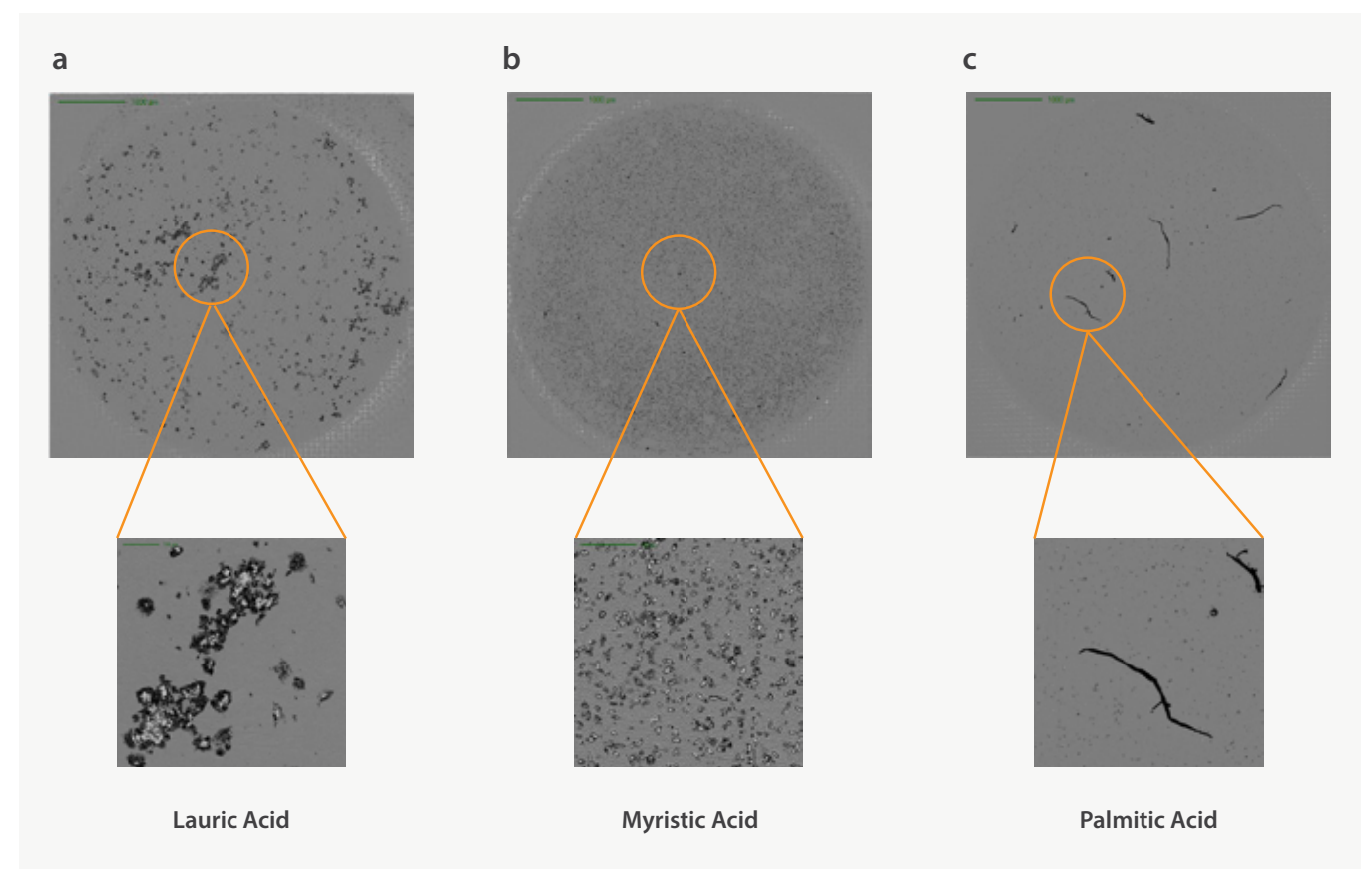


FIGURE 2: Morphological appearance of different fatty acids particles using brightfield image on the Aura. (a) Large, irregular particles of 150 µM of lauric acid. (b) Smaller particles of 87.6 μM of myristic acid. (c) Fibril-like particles of 31.2 μM of palmitic acid.



C₁₆ even reaching the saturation point (255-pixel intensities). In contrast, none of the labeled hlgG particles fluoresce above the background, with all their intensity values measuring along the background baseline (Figure 4b). We also see in Figure 4a that the larger the particle the larger the fluorescence intensity, likely due to the larger number of dye binding sites being filled.

Free Fatty Acid Limit of Detection (LOD) and Quantitation (LOQ) in the Presence of hlgG

We then determined the LOD and LOQ values of FFAs in the presence of hlgG. Figure 5 shows the FL2 particle counts ($>5 \mu m$) of a mixture of 0.049 mg/mL hlgG (~0.31 μM) and 9 different concentrations of 3FFAs. Both, hlgG and the supersaturated mixture of the three fatty acids were prepared

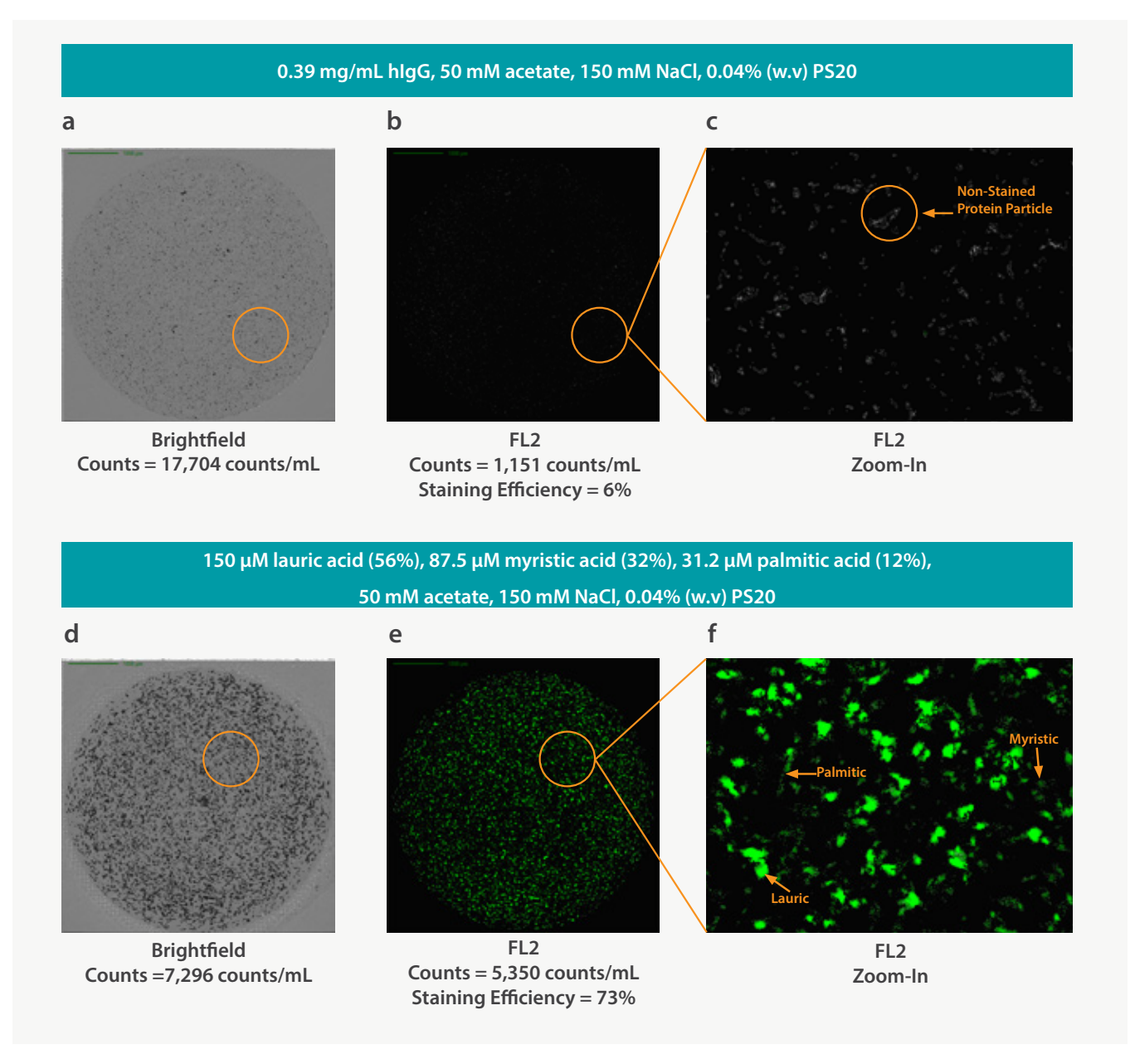


FIGURE 3: Images showing BODIPY FL C₁₆ staining of IgG (negative control) and 3FFAs (positive control) (a) BF full well image of hIgG particles. (b, c) Combined FL2 images showing hIgG particles that were stained (no fluorescence). (d) BF full well image of 3FFAs. (e, f) Combined FL2 images showing 3FFAs particles that were stained (strong fluorescence).

with acetate buffer containing 0.01% (w/v) PS20. For simplicity, and because lauric acid is the major component of PS20, we graphed the concentration of lauric acid in the x-axis. The concentration of hlgG was kept constant at 0.049 mg/mL in all samples while the a titration series of the 3FFAs from 150 µM to 0.6 µM was created using 2-two serial dilutions.

Figure 5a, clearly demonstrats that the LOD of the 3FFA sample is 9.38 µM (>2183 counts/mL) and the LOQ is $18.75 \,\mu\text{M}$ (>2976 counts/mL). The linear fit of the logarithm of FL2 counts and the lauric acid's concentration yielded a straight line of $R^2 = 0.9864$ with an intercept of 1.828 ± 0.022 (negative control of 1682 ± 26 counts/mL) (Figure 5b).

Figure 6 reveals that at a relative concentration of 9.38 µM lauric acid, the particles of the 3FFA mixture (Figure 6a) stains significantly more by BODIPY FL C₁₆with respect to the negative control (0.049 mg/mL hlgG) (Figure 6b). The power of the Aura polysorbate degradation assay is that the particle ID is visually

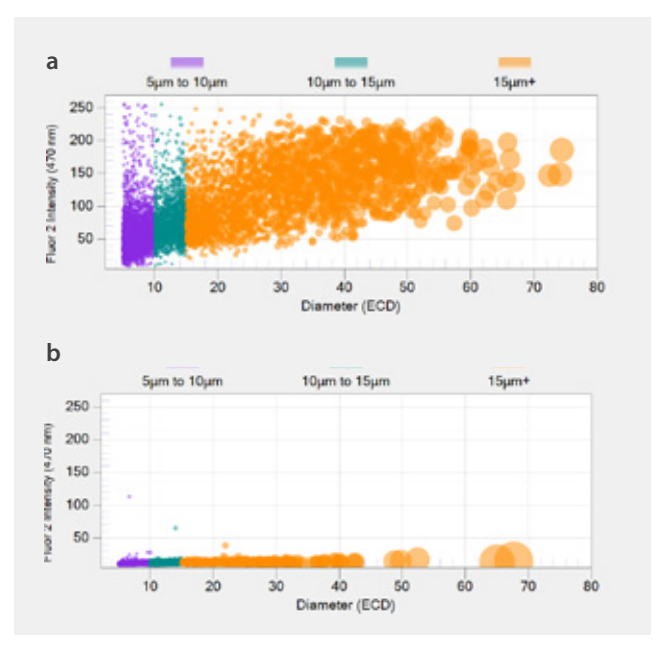


FIGURE 4: Scatter plots showing the FL2 signal (average particle FL2 intensity) vs diameter (ECD). Color represents particle size bins. (a) PS20+3FFAs and (b) PS20+hlgG.

verifiable by observing the resulting combined BF / FL images. Notice that in Figure 6b when hlgG is mixed with 3FFAs, more particles fluoresced more strongly than the controls shown in Figure 6a. This observation supports the data shown in Figure **5a**, where the detection of 3FFAs is possible above 9.38 µM lauric acid. These limits of detection are more sensitive and are well in line with the solution phase polysorbate assays reported in the literature.8

Conclusions

The Aura can easily detect the major degradation components of PS20 in protein-containing samples at any stage of the drug manufacturing process. The method only requires 5 µL of sample, is specific

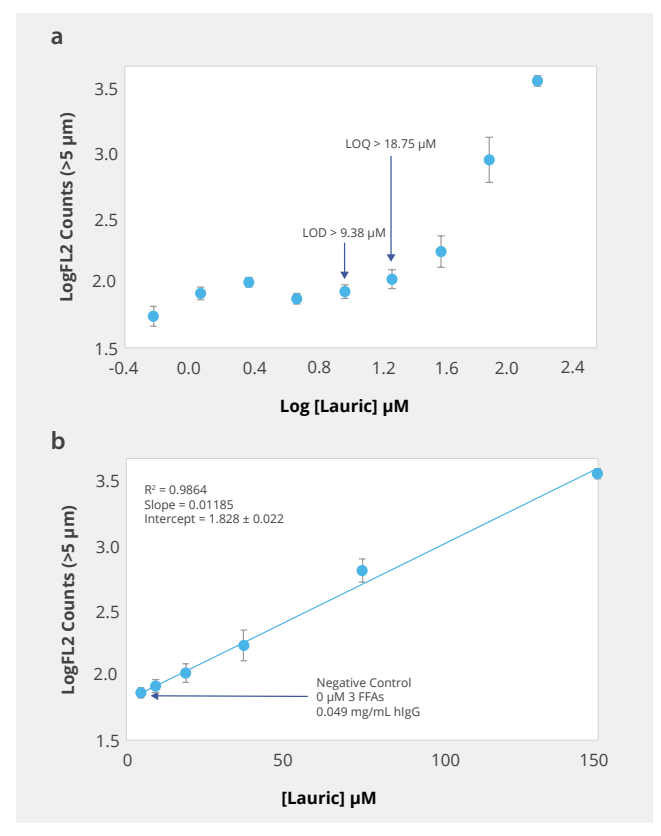


FIGURE 5: FL2 particle counts of the mixture hlgG+3FFAs determined after adding BODIPY FL C_{16} . The blue line represents the linear fit of the Log FL2 counts and concentration of lauric acid. (a) Log-Log plot of the FL2 particle counts of 9 different concentrations of 3FFAs. (b) Linear fit of the logarithm of the FL2 counts vs concentration of 3FFAs (expressed as concentration of lauric acid).



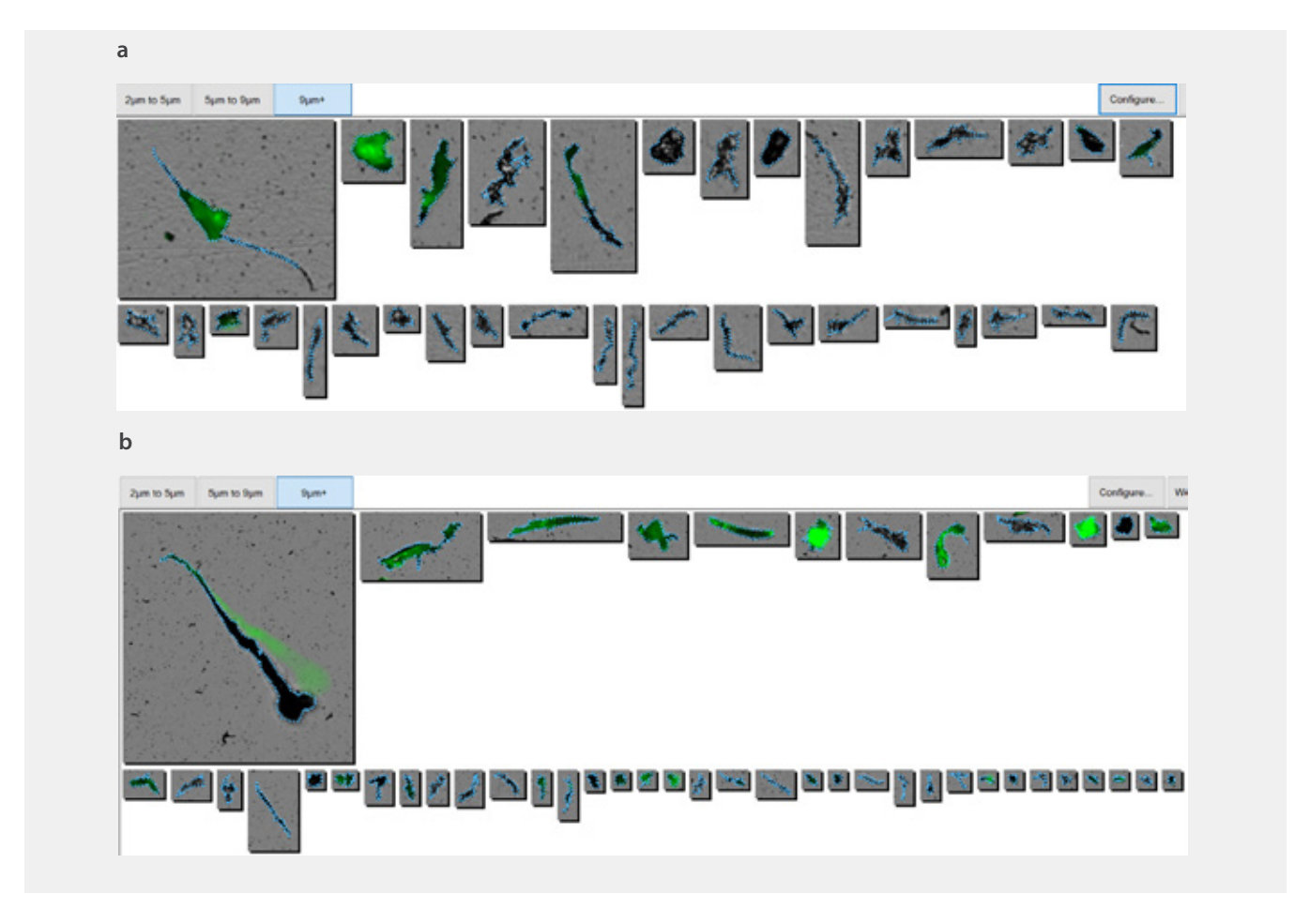


FIGURE 6: Image gallery showing particle staining by BODIPY FL C_{16} . (a) Particles of the negative control (0.049 mg/mL hlgG). (b) Particles of the negative control (0.049 mg/mL hlgG). cles of the mixture hlgG+3FFAs at a relative concentration of 9.38 µM lauric acid.

and sensitive, and can analyze 96 samples in just a few hours, far outperforming other techniques. The Aura can also identify and differentiate the key degraded particulates from polysorbate formulation by their distinguishable shape, appearance,

and specific labeling with BODIPY FL C₁₆. The Aura polysorbate assay can detect FFAs at concentrations relative to lauric acid above 9.38 µM (>2183 counts/mL) and quantitate above 18.75 μM (>2976 counts/mL).

References

- 7. Vaclaw C, et al., Impact of Polysorbate 80 Grade on the Interfacial Properties and Interfacial Stress Induced Subvisible Particle Formation in Monoclonal Antibodies. J Pharm Sci. 2020, 110 (2), 746-759.
- 8. Dwivedi M, et al., Acidic and Alkaline Hydrolysis of Polysorbates Under Aqueous Conditions. Eur J Pharm Sci. 2020, 144, 105211.
- Doshi N, et al., Understanding Particle Formation: Solubility of Free Fatty Acids as Polysorbate 20 Degradation Byproducts in Therapeutic Monoclonal Antibody Formulations. Mol Pharm. 2015, 12 (11), 3792-3804.
- 10. Glücklich N, et al., An In-Depth Examination of Fatty Acid Solubility Limits in Biotherapeutic Protein Formulations Containing Polysorbate 20 and Polysorbate 80. Int J Pharm. 2020, 591, 119934.

- 11. Saggu M, et al., Identification of Subvisible Particles in Biopharmaceutical Formulations Using Raman Spectroscopy Provides Insight Into Polysorbate 20 Degradation Pathway. Pharm Res. 2015, 32(9), 2877–2888.
- 12. Doshi N, et al., Improving Prediction of Free Fatty Acid Particle Formation in Biopharmaceutical Drug Products: Incorporating Ester Distribution during Polysorbate 20 Degradation. Mol Pharm. 2020, 17 (11), 4354-4363.
- 13. Doshi N. *et al.*, Evaluation of Super Refined™ Polysorbate 20 With Respect to Polysorbate Degradation, Particle Formation and Protein Stability. J Pharm Sci. 2020, 109 (10), 2986-2995.
- 14. Martos A, et. al, Novel High-Throughput Assay for Polysorbate Quantification in Biopharmaceutical Products by Using the Fluorescent Dye Dil. J of Pharm Sci. 2020, 109, 646.



Protein Degradation and Particle Formation Control Strategies



BY GAIL DUTTON

nterfacial stress analysis is an important step when evaluating the ability of various polysorbates (PS) to mitigate formation of subvisible and visible protein particles at the air/water interface of monoclonal antibody formulations.

In a recent paper, researchers led by Prajnaparamita Dhar, PhD, professor, chemical and petroleum engineering, University of Kansas, compared the effects of PS20 and PS80 on the interfacial properties and rate of particle formation in two immunoglobulin G1 molecules.

For all the mixtures, adding surfactants at concentrations of 100 ppm—well above the critical micelle concentration (CMC)—prevented adsorption of the protein to the air/water interface. At lower PS concentrations, that ability varied according to the surfactant and the protein.

For example, with PS concentrations below the CMC, the protein seemed to co-adsorb at the air/water interface. Dhar and colleagues surmise the lower surfactant concentrations failed to fully saturate the surface of the



interface or that both molecules are competing for that interface.

"Our results also suggest that the amount of surfactant needed to prevent adsorption of the mAb to the air/water interface also depends on the concentration of molecules competing for the air/water interface," they wrote.

Dilational Stress Affects Competitive Adsorption

Applying dilatational stress to the air/water interface affects "the competitive adsorption between the surfactant and the mAb molecules (that are) competing for any new area that is generated during the start of every expansion cycle," according to the paper. The outcome is determined by the rate of adsorption of the surfactant and the mAb molecules at the air/water interface.

Although PS20 and PS80 were each effective, PS20 appeared significantly better at preventing large particle formulation.

When specifically addressing the air/water interface, however, protein particle formation varied by solution and surfactant. For example, the mAb 2/ surfactant solutions all reduced the number of particles formed at the interface but, for mAb1/ surfactant solutions, protein particles actually increased for the 100 ppm PS20 solutions.

The researchers hypothesize that differences in adsorption rates determine how many protein complexes are formed. Additional possibilities are that micelles may promote protein particle formulation, or that the surfactants interact differently with the mAbs, causing surfactant/protein complexes to form in one, but not the other.

To determine which PS best prevents protein particle formation at the air/water interface for any particular formulation, the researchers advocate analyzing spatial pressure versus time kinetics, and spatial pressure versus interfacial area isotherms. Ultimately, the choice of surfactant may depend on the nature of the mAb.



Step into the Future

Experience a new era of biologics screening with Aura PTx - a high-throughput system that combines protein stability analysis, characterization, and assays into one user-friendly tool.

